Title	Statistical atlas based registration and planning for ablating bone tumors in minimally invasive interventions
Author(s)	Kang, X; Ren, HL; Li, J; Yau, WP
Citation	The 2012 IEEE International Conference on Robotics and Biomimetics (ROBIO 2012), Guangzhou, China, 11-14 December 2012. In IEEE International Conference on Robotics and Biomimetics Proceedings, 2012, p. 606-611, article no. 6491033
Issued Date	
URL	http://hdl.handle.net/10722/186870
Rights	IEEE International Conference on Robotics and Biomimetics Proceedings. Copyright © IEEE.

Proceedings of the 2012 IEEE
International Conference on Robotics and Biomimetics
December 11-14, 2012, Guangzhou, China

Statistical Atlas Based Registration and Planning for Ablating Bone Tumors in Minimally Invasive Interventions

Xin Kang[1], PhD, *Member IEEE;* Hongliang Ren[2*], PhD, *Member, IEEE*; and Jing Li[3], MD, PhD; Wai-Pan Yau[4], MD

***Abstract*— Bone tumor ablation has been a viable treatment in a minimally invasive way compared with surgical resections. In this paper, two key challenges in the computer-assisted bone tumor ablation have been addressed: 1) establishing the spatial transformation of patient's tumor with respect to a global map of the patient using a minimum number of intra-operative images and 2) optimal treatment planning for large tumors. Statistical atlas is employed to construct the global reference map. The atlas is deformably registered to a pair of intra-operative fluoroscopy images, constructing a patient-specific model, in order to reduce the radiation exposure to the sensitive patients such as pregnant and infants. The optimal treatment planning system incorporates clinical constraints on ablations and trajectories using a multiple objective optimization, which obtains optimal trajectory planning and ablation coverage using integer programming. The proposed system is presented and validated by experiments.**

***Index Terms*— Deformable registration, Ablation, Statistical Atlas, Planning, Optimization.**

I. Introduction

According to the statistics from American Academy of Neurological and Orthopaedic Surgeons, though bone cancer is not as common as other types of cancers, it has higher occurrence rate in children and youth, which tremendously devastates the entire life quality of patients. Invasive treatments together with high radiation exposure can make this even worse, so it's of great importance to develop minimally invasive interventions with minimal radiation exposure. Percutaneous radiofrequency ablation (RFA) has emerged as a routinely used technique for the minimally invasive treatment of numerous organ cancers [1], such as tumors in bone, lung or liver.

In practice, clinicians are mostly facing two challenges in minimally invasive interventions – how to accurately ablate the tumor with minimal radiation exposure to the patient, and how to make multiple ablations efficiently covering a large tumor. Manual treatment planning and execution is dependent on the operator's experiences and relies on a trial-and-error approach. This is error-prone and time-consuming without the assistance of planning and navigation. Planning could be done using the patient pre-operative CT images. However, such CT images are not always available since taking CT scan is not suitable for all patients due to its high radiation exposure.

To address the aforementioned key challenges, this paper focuses on a statistical atlas based registration approach for constructing patient-specific models with minimal radiations (two fluoroscopy shots in this article) and a multiple-objective optimization for ablation planning. These two aspects are the major novel contributions of this paper: statistical atlas based registration and planning, as depicted in Fig. 1.

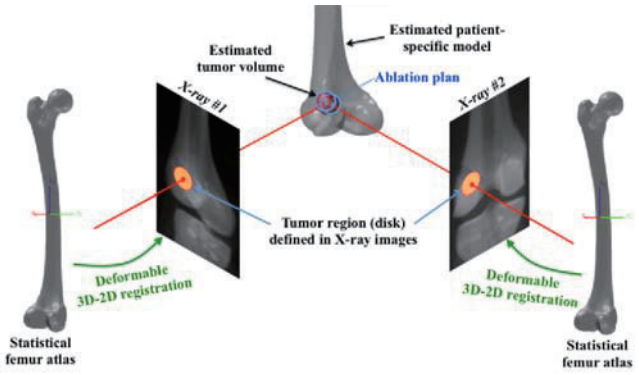

Fig. 1. The diagram of the proposed atlas-based registration and planning system for tumor ablation.

There are three advantages of the proposed method: 1) no same-patient CT scan is required, which reduces the radiation exposure to the patient as well as to the physicians; 2) the patient-specific model and its spatial transformation to a pair of intra-operative X-ray images are optimized simultaneously rather than sequentially, which potentially increases the accuracies of the model and registration; and 3) the treatment planning module yields optimal overlapping ablation plans based on the constructed patient-specific anatomical model and tumor model. Accurate ablation delivery can be achieved by incorporating the current system with other robotic devices.

The rest of this paper is organized as follows. Section II summarizes the challenges, significance and related work in

This work was supported in part by the Singapore Academic Research Fund, under Grant R-397-000-139-133 and NUS Teaching Enhancement Grant C-397-000-039-001 awarded to Dr. Hongliang REN.

[1]Bioengineering Initiative, Sheikh Zayed Institute for Pediatric Surgical Innovation, Children's National Medical Center, Washington D.C, 20010, USA. (email: xkang@cnmc.org).

[2*]Corresponding Author, Department of Bioengineering, National University of Singapore, Singapore, 117576 (email: ren@nus.edu.sg).

[3]Department of Orthopaedics, Xijing Hospital and The Fourth Military Medical University, Xian, China.

[4]Department of Orthopaedics and Traumatology, The University of Hong Kong, Hong Kong, China (email: peterwpy@hkucc.hku.hk).

978-1-4673-2127-3/12/$31.00 © 2012 IEEE

registration and planning, particularly for tumor ablation. Section III presents the proposed approach, which is validated in Section IV. Finally Section V concludes the paper.

II. Significance And Related Work

A. *Registration and Reconstruction of Patient-Specific Models*

Registration is a key step in accurate image-guided surgeries [2] [3] [4] to get the transformation from intra-operative patient anatomy to pre-operative models or statistical population models. There is a large body of research on image registration using various modalities.

However, the construction of 3D surface models of patients' anatomy from one calibrated 2D images is a very challenging task. Some *a-priori* knowledge on the geometric structure of the anatomy is often required to constrain the ill-posed nature of the problem. Making use of statistical atlases is an alternative for taking this *a priori* information into considerations because an atlas can effectively capture the mean and the variations of a given population.

Various methods have been proposed for constructing a patient-specific model from one image using statistical atlases. Intensity-based methods (e.g., [5]) perform deformable 3D-2D registration between X-ray images and digitally reconstructed radiographs (DRRs) generated from a statistical volumetric atlas, by optimizing certain intensity similarity. However, a statistical volumetric atlas is not easy to build and the deformable registration using it needs to optimize ultra-high dimensional nonlinear object functions.

Feature-based methods employed statistical shape atlas and minimize some distance between edges extracted in the image and model silhouette. A large amount of methods (e.g., [6] [7] [8] [9]) achieved this sequentially: 1) rigid 3D-2D registration using the mean shape of the atlas; 2) global deformation using the variations of the atlas and the fix transformation obtained in step 1); and 3) local deformation of the model obtained in step 2) using free-form deformation model.

Zheng et al. [10], [11] proposed to address the problem by adapting the ICP algorithm. They proposed a three-stage process: scaled rigid registration, statistical instantiation, and regularized local deformation. The scaled rigid transformation was estimated using ICP from paired ray-model pairs between the mean shape of the PDM and the X-ray images. Statistical instantiation is an adapted ICP algorithm, aiming to refine the rigid registration. In the regularized shape deformation, the local deformation was treated as a free-form deformation and formulated as a constraint least-squares surface fitting problem using 3D point correspondences established before, wherein the 3D thin-plate spline was used to constrain the smoothness of deformation [14]. After rigidly aligning the mean shape of the PDM to the image contour, the shape parameters were estimated using the conjugate gradient method. Clean image contours are need for this method. The ICP algorithm plays an important role in the two registration parts and explicit point correspondences are necessities for the registration as well as the deformation.

Hurvitz and Joskowicz [15] proposed to establish explicit paired correspondences by performing 2D-2D intensity-based deformable registration between the X-ray images and DRRs, aiming to avoid edge detection and to reduce the probability of mismatching. The DRRs were generated using a CT-like atlas. The 2D image deformation was modelled using a B-spline transformation, which was estimated using gradient descent. The estimated B-spline transformation was then applied to the contour points of the DRR to calculate the point-ray pairs in a way similar to the approach in [14]. The major difference lies in the way of establishing the paired point correspondences. Instead of extracting image contours from the DRRs, the projections of uniformly spaced sample points on the apparent contour of the template surface model were used. Visual rays were calculated for each sample point using the estimated pose. Finally, by minimizing the distances of these point-ray pairs, new atlas pose and shape parameters were estimated using pattern search algorithm. To establish paired point correspondences, a gradient descent optimization method was used for 2D-2D intensity-based deformable registration. To initialize whole procedure, manually marked landmarks in each X-ray image were used. The construction accuracy is governed by the intensity-based 2D-2D registration as well as the sampling scheme.

Most recently, a method was proposed in [16] by employing an orientation weighting [17] to diminish the influence of false correspondences. Using the point-ray distance, it minimizes the sum of back-projection error in 3D as so doing in [6]. The back-projection error is multiplied by the weight defined in 2D as the cosine of the angle from the projected surface normal to the image gradient at the corresponding edge location, aiming to suppress the paired correspondences with large angle difference. This method in essence is an ICP-like method that takes the closest point on the edge map as correspondences. The surface reconstruction was performed via two sequential stages: 1) rigid registration using the mean shape of atlas and 2) shape estimation using the estimated transformation. The optimization problems were solved by using preconditioned conjugate gradients in a trust region approach.

B. *Treatment planning for tumor ablation*

Baegert [18] employed a visibility graph method to optimize entry point and no-fly zone, but they did not address overlapping ablation issues. Overlapping spherical ablations have been studied by Dodd and Chen [19] [20]. Dodd [20] developed geometrical models to cover spherical tumors and Chen [19] explores an alternative approach by inscribing a regular polyhedron in the target sphere and circumscribing each face of the polyhedron with an ablation sphere. Villard et al. [18] used a local search optimization technique, which may not yield global optimal solutions.

This paper differs from the related studies such as [18] [19] [20], in three aspects: 1) the use of patient-specific models derived from a statistical atlas of the bone, which ensures the minimal radiation exposure to both patient and physician, 2) a treatment planning method based on decoupled mathematical programming for optimizing overlapping ablations and 3) the addressing of clinical constraints of minimizing the number of probe punctures to ensure minimal invasiveness, minimizing the number of ablations while giving complete coverage over the tumor, and avoiding critical objects such as neurovascular bundles.

III. The Propose Method

A. *Image-Guided Bone Tumor Ablation*

The statistical atlas guidance system for tumor ablation consists of three key modules (see Fig. 2): 1) statistical atlas building, 2) deformable 3D-2D registration for simultaneous pose estimation and patient-specific model construction, and 3) treatment planning optimization for execution.

Section III.B presents the approach for building a statistical atlas, *AL*, as a populational model. Section III.C describes the proposed method for registering the statistical atlas to a single X-ray, X_R, to get the atlas to patient transformation, T_F, as well as constructing the patient-specific model. The T_F is a 6-DOF transformation, called "pose", which includes a rotation R and a translation $\boldsymbol{t}$. Finally the transformation, T_F, will be used to map the tumor in X-ray to its spatial location residing in statistical atlas. The ablation planning approach described in Section III.D will be utilized to get optimal tumor ablation coverage while avoiding critical non-fly-zone.

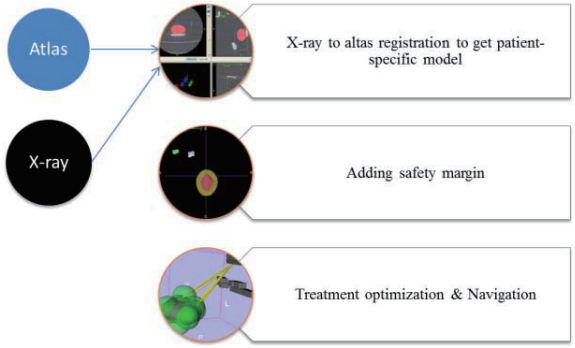

Fig. 2 Diagram of the statistical atlas guided tumor ablation system.

B. *The Statistical Atlas*

Statistical atlases have been used in various applications to characterize differences between individuals in a population. In terms of building patient-specific models, they provide a natural and meaningful manner to regularize the automatic generation of plausible instances, which otherwise is ill-posed. Approaches of constructing, training and using statistical models in different of applications can be found in [21,22].

To characterize shape variations, a statistical shape atlas is commonly constructed using PDM [23], according to the standard procedures in the principle component analysis (PCA) of shapes. Consequently, a mean shape $S^{[0]}$, modes of shape variation $e^{[k]}$ and shape variation λ_t are obtained. A valid shape instance can be constructed by a linear combination of the mean shape and the first K dominant modes. In practice, the shape of a 3D object is commonly given as a triangulated surface mesh with M vertices. It is convenient to represent a shape instance using vertices. Therefore, the m-th vertex on an instance shape can be written as,

$$\boldsymbol{X}_m \approx \boldsymbol{X}_m^{[0]} + \sum_{k=1}^{K} \alpha_k \boldsymbol{e}_m^{[k]}, \quad m = 1, \ldots, M.$$

where $X^{[0]}$ is the m-th vertex on the mean shape $S^{[0]}$ and α_k is the coefficient of the k-th mode.

Commonly, α_k is constrained by applying the limit of $\pm 3\lambda_k$, assuming all modes are independent [24]. A more accurate estimate of the shape parameter $\boldsymbol{\alpha} = (\alpha_1, \ldots, \alpha_K)^T$ can be obtained using multivariate Gaussian models [23].

C. *Simultaneous 3D-2D Registration and Patient-Specific Model Construction*

Instead of using the same-patient pre-operative CT images, a patient-specific model is built from a single X-ray image via a deformable 3D-2D registration that makes use of statistical atlas. For the guidance, the pose of the patient-specific model with respect to the patient on the operation table is required. In fact, the registration and modeling are two coupled problems: the registration needs an accurate model while the accurate modeling requires an accurate pose.

Unlike the methods in literature that perform registration using the mean shape $S^{[0]}$ and then construct a plausible model by fixing the transformation parameters, the registration and model construction are optimized simultaneous in our method. This is achieved by minimizing the objective function

$$\sum_{m=1}^{M} \sum_{n=1}^{N} d_{mn}^2 + \rho \sum_{k=1}^{K} \frac{\alpha_k^2}{\lambda_k^2}. \qquad (1)$$

$$d_{mn} = \sqrt{p_{mn}} \left\| V_n \left[\boldsymbol{c}_n - \left(R\boldsymbol{X}_m^{(0)} + \sum_{k=1}^{K} \alpha_k R\boldsymbol{e}_m^{(k)} + \boldsymbol{t} \right) \right] \right\|$$

The solution of (1) is referred to as the *maximum penalized likelihood estimate* (MPLE) since the shape parameter $\boldsymbol{\alpha}$ used for registration in the first term needs to fulfill the constraints from its prior probability distribution in the second term. Specifically, the first term is the sum of Euclidean distances between the N line-of-sight and the estimated shape weighted by the posterior correspondence probabilities, p_{mn}. The second term is the Mahalanobis distance of the estimated shape from the mean shape, which ensures that the estimate shape is legitimate in terms of the statistical plausibility. The free parameter ρ>0 modulates the contribution of the penalty term.

In (1) d_{mn} is the weighted distance of the vertices X_m to the line (c_n, v_n) passing through the center of perspective c_n and having the direction v_n. Instead of using the inverted distances as so doing in the methods in literature, the weights are the correspondence probabilities. V_n is the skew symmetric matrix implementing the vector cross product with v_n, and p_{mn} is the correspondence probability.

Without the need for establishing paired correspondences, the simultaneous 3D-2D deformable registration and patient-specific model construction are solved by adapting the "one-step-later" (OSL) algorithm [25]. Specifically, the 3D-2D deformable registration is achieved using the method [26] [27] that couples particle swarm optimization (PSO) with expectation maximization (EM). The proposed method stops when the OSL is converged or the maximal number of iteration is reached. The patient-specific model and its pose with respect to the given X-ray are obtained simultaneously, rather than sequentially.

D. *The Closed-form Solution of The Shape Parameter*

As the estimation of $\boldsymbol{\alpha}$ is carried out within the M-step, a closed-form optimal solution for it is preferred, considering the computational efficiency.

By further defining

$$\boldsymbol{d}_{mn}^{(0)} = \sqrt{p_{mn}} V_n \left(\boldsymbol{c}_n - R\boldsymbol{X}_m^{(0)} - \boldsymbol{t} \right),$$

$$\boldsymbol{q}_{mn}^{(k)} = \sqrt{p_{mn}} V_n R\boldsymbol{e}_m^{(k)}. \qquad (2)$$

the objective function (1) can be written in the form of a linear

system of the shape parameter as A$\boldsymbol{\alpha}$ = b with

$$\boldsymbol{A} = \sum_{m=1}^{M}\sum_{n=1}^{N} Q_{mn}^{T} Q_{mn} + \frac{1-\rho}{\rho}\Lambda^{-1}, \quad \boldsymbol{b} = \sum_{n=1}^{N} Q_{mn}^{T}\boldsymbol{d}_{mn}^{(0)}.$$
$$Q_{mn} = \sqrt{p_{mn}}\left[\boldsymbol{q}_{mn}^{(1)}, \ldots, \boldsymbol{q}_{mn}^{(K)}\right]. \quad (3)$$

where $\Lambda = diag(\lambda)$ is a diagonal matrix with $\boldsymbol{\lambda} = [\lambda_1^2, \ldots, \lambda_K^2]^T$.

This results in a linear equation system over the unknown shape parameter $\boldsymbol{\alpha}$, which can be solved using standard linear equation system solvers such as QR decomposition. This closed-form solution enables the real-time estimation of shape parameter and hence facilitates the use of the complete set of eigenvectors for shape estimation.

E. *The Estimation of Tumor Region Center*

In order to estimate the center of a spherical tumor region, two intra-operative fluoroscopic images are used. In the worst case where the imaging device is not tracked, the proposed 3D-2D deformable registration is performed using each image respectively, as illustrated in Fig. 1. Then the 3D center of the spherical tumor region is calculated via triangulation using the two estimated transformations. Consequently, the center of the tumor region within the constructed patient-specific model is ready for use in the planning.

F. *The Optimal Planning*

By far, the patient specific bone models together with tumor models are derived from the statistical atlas as described in the last section. Then the tumor treatment optimization module derives optimal probe insertion trajectories as well as optimal placement locations of ablation electrode. The optimization need to satisfy the constraints of fulfilling complete tumor coverage, starting from specified entry points, avoiding critical no-fly zone, and minimizing the number of ablations and skin punctures. The no-fly zone and entry regions are generally specified by the clinicians.

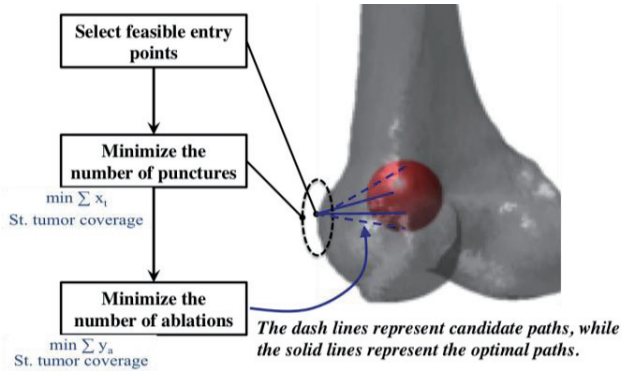

Fig. 3 The optimal treatment planning is achieved using decomposed multiple-objective mathematical programming. Starting from feasible entry points to effectively avoid the critical no-fly zone, the optimal needle trajectories should result in the minimum number of skin punctures as well as the minimum number of ablations.

As a common practice, the ablation electrode is modeled to generate an ablation sphere of radius, *R*, which is given by the manufacturer specification. The multiple-constraint problem is formulated as a sequence of decomposed multiple-objective integer programming sub-problems as shown in Fig. 3.

Minimal punctures are required for the minimally invasive intervention that leads to multiple ablations using a minimal number of trajectories. The trajectories are commonly planned preoperatively. In this paper, the planning is achieved by minimizing the number of trajectories and the number of ablations as illustrated in Fig. 3.

SUBJECT TO EXPERIMENTS

The proposed method for tumor ablation was validated using simulation studies. High-resolution CT images of 19 normal adult cadaveric femurs were acquired. Each slice is 512x512 pixels with pixel size of 0.703 mm and thickness of 0.625mm. The ground-truth model of each cadaveric femur was obtained by manually segmenting its CT using Analyze (AnalyzDirect Inc., Kansas, USA). Then, the "leave-one-out" evaluations were carried out using these CT reconstructions of 19 cadaveric femurs. That is, one CT was chosen as the patient data while the rest 18 CTs were used to build a statistical atlas. Doing so is clinical meaningful; in practice, it is unlikely that the patient's CT is available for atlas building.

A. *Patient Specific Model based on Statistical Atlas*

The construction error of the patient-specific model was measured using surface-to-surface distance, which is defined as the Hausdorff distance of the constructed surface model to the ground-truth surface model.

One typical constructed surface model using the proposed method is shown in Fig. 4. On the top, the surface rendering of the reconstructed femur is shown in side, top and front view. On the bottom left shows the histogram of the construction errors. As can be seen, the maximal error was 2.34 mm and the mean was 0.84 mm. To depict the spatial distribution of the construction errors, on bottom right, they are visualized on the constructed model in the color-coded manner: the warmer the color, the higher the error.

B. *Ablation Planning Using the Patient Specific Model*

An artificial bone tumor of 24 mm diameter was generated and registered to the patient-specific model. An ablation probe of 20 mm diameter was used for radiofrequency ablation, assuming the ablation electrode can kill a spherical space with multiple tines.

The multiple candidate plans from the optimization module are evaluated both numerically and visually to verify the coverage rate and feasibility for execution. The numerical evaluation module calculates the volumetric overlap between the tumor and multiple ablation spheres placed at the planned locations. Specifically, the Ablation Coverage is given by

$$\text{Ablation Coverage} = \text{Ablations} \cap \text{Tumor} / \text{Tumor}. \quad (6)$$

The augmented reality module displays an overlay of the 3D planned spheres within the constructed 3D patient-specific model, presenting a complete view (Fig. 5) to clinicians to examine how the tumor is covered by each ablation. This is especially useful when the clinician needs to select the best plan from multiple candidate plans.

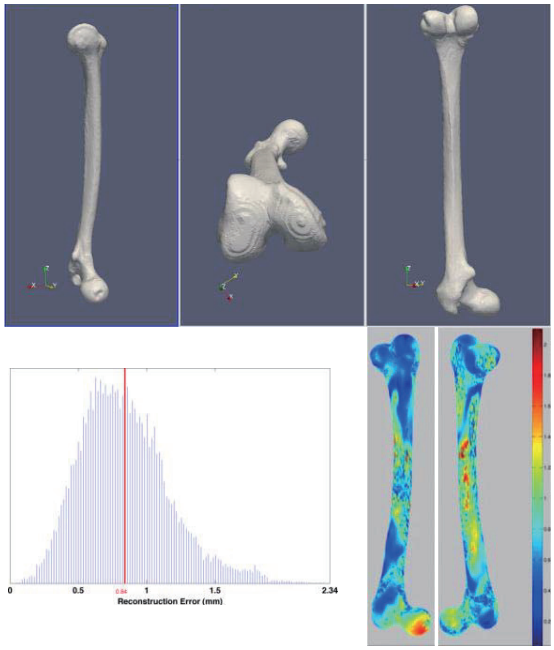

Fig. 4. The patient-specific model and its construction errors.

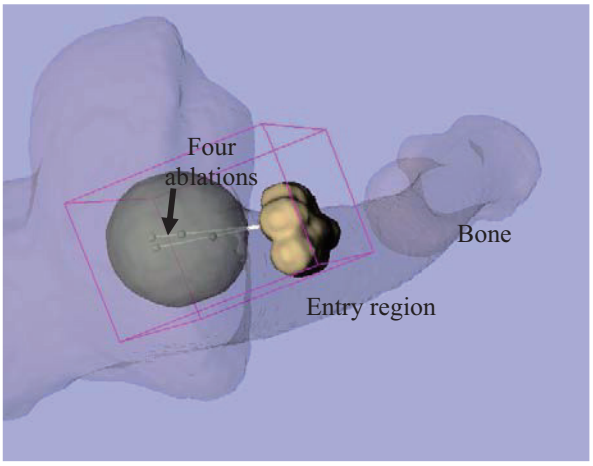

Fig. 5. Visualization of the patient specific model and one selected plan for multiple overlapping ablations. The four locations for ablations are represented by the four beads, which are connected by two trajectories.

TABLE I: STATISTICAL MEASURES OF THE CANDIDATE PLANS FOR SIMULATED TUMOR SPHERE OF DIAMETER 24 MM ABLATED BY 20 MM DIAMETER PROBE

Plan ID	Ablation Coverage	# Ablations	# Trajectories
1	1	6	2
2	1	6	2
3	1	4	2
4	1	4	2

For the four candidate treatment plans, their numerical coverage evaluation is shown in Tabel I. Note that plan 1 and plan 2 are different in terms of ablation locations as well as over treatment rate, even though they both have complete coverage over the tumor, 2 trajectories and 6 ablations. The plan 3 and plan 4 are different in this way. The augmented visualization of one of the candidate plans is shown in Fig. 5.

In the planning experiment, if an ablation sphere of 30 mm diameter can be generated by the probe, then only 1 ablation is required for killing the tumor.

The experimental results have demonstrated the feasibility of applying the proposed planning system to phantom study as well as patient study. Adequate coverage on the tumor region can be achieved using the minimum number of punctures and ablations.

V. CONCLUSION

This paper has demonstrated the feasibility of the proposed method for atlas-based, image-guided large bone tumor ablation. The proposed method is able to simultaneously build a statistical plausible patient-specific model and achieve 3D-2D deformable registration, using only one image. Its extension to the use of multiple images is straightforward when the tracking of intraoperative imager (e.g., C-arm) is available. In addition, the proposed optimal planning approach is able to the cover large tumors in a minimally invasive way.

Future work includes validations of the proposed method using phantom and animal studies. With the capability of constructing patient-specific model from a couple of images using statistical atlas for planning, another future direction is to develop intra-operative surgical guidance navigation system based on the system proposed in this paper.

VI. REFERENCES

[1] M.J. Howenstein and K.T. Sato, "Complications of Radiofrequency Ablation of Hepatic, Pulmonary, and Renal Neoplasms," in *Seminars in interventional radiology*, vol. 27, 2010, pp. 285-295.

[2] Hongliang Ren, Denis Rank, Martin Merdes, Jan Stallkamp, and Peter Kazanzides, "A Wireless Integrated Electromagnetic and Inertial Navigation System for Image-Guided Surgery," *IEEE/ASME Transactions on Mechatronics, submitted*, 2011.

[3] Hongliang Ren and Peter Kazanzides, "A Paired-Orientation Alignment Problem in a Hybrid Tracking System for Computer Assisted Surgery," *Journal of Intelligent and Robotic Systems*, vol. 63, pp. 151-161, 2011, 10.1007/s10846-010-9475-y. [Online]. http://dx.doi.org/10.1007/s10846-010-9475-y

[4] Hongliang Ren, Denis Rank, Martin Merdes, Jan Stallkamp, and Peter Kazanzides, "Multi-Sensor Data Fusion in An Integrated Tracking System for Endoscopic Surgery," *IEEE Transactions on Information Technology in Biomedicine*, vol. 16, no. 1, pp. 106-111, 2012.

[5] Jianhua Yao and R. Taylor, "Assessing accuracy factors in deformable 2D/3D medical image registration using a statistical pelvis model," in *Ninth IEEE International Conference on Computer Vision*, oct. 2003, pp. 1329 -1334 vol.2.

[6] M. Fleute and S. Lavallee, "Nonrigid 3-D/2-D registration of images using statistical models," in *MICCAI'99*, vol. LNCS 1679, Berlin Heidelberg, 1999, pp. 138-147.

[7] H. Lamecker, T.H. Wenckebach, and H.-C. Hege,

"Atlas-based 3D-Shape Reconstruction from X-Ray Images," in *18th International Conference on Pattern Recognition, 2006. ICPR 2006.*, vol. 1, 0-0 2006, pp. 371-374.

[8] S. Benameur, M. Mignotte, H. Labelle, and J.A. De Guise, "A hierarchical statistical modeling approach for the unsupervised 3-D biplanar reconstruction of the scoliotic spine," *IEEE Trans Biomed Engineering*, vol. 52, no. 12, pp. 2041-2057, dec. 2005.

[9] S. Benameur et al., "3D biplanar reconstruction of scoliotic vertebrae using statistical models," in *Proceedings of the 2001 IEEE Computer Society Conference on Computer Vision and Pattern Recognition, 2001* , vol. 2, 2001, pp. II-577 - II-582 vol.2.

[10] Guoyan Zheng, "Statistical shape model-based reconstruction of a scaled, patient-specific surface model of the pelvis from a single standard AP x-ray radiograph," *Medical Physics*, vol. 37, no. 4, pp. 1424-1439, 2010.

[11] Guoyan Zheng, "Statistically Deformable 2D/3D Registration for Accurate Determination of Post-operative Cup Orientation from Single Standard X-ray Radiograph," in *Medical Image Computing and Computer-Assisted Intervention (MICCAI 2009)*, Guang-Zhong Yang et al., Eds.: Springer Berlin / Heidelberg, 2009, vol. 5761, pp. 820-827.

[12] Guoyan Zheng, "A Novel 3D/2D Correspondence Building Method for Anatomy-Based Registration," in *Biomedical Image Registration*, Josien Pluim, B. Likar, and Frans Gerritsen, Eds.: Springer Berlin / Heidelberg, 2006, vol. 4057, pp. 75-83.

[13] Kumar T. Rajamani et al., "Statistical deformable bone models for robust 3D surface extrapolation from sparse data," *Medical Image Analysis*, vol. 11, no. 2, pp. 99-109, 2007.

[14] Guoyan Zheng et al., "Accurate and Robust Reconstruction of a Surface Model of the Proximal Femur From Sparse-Point Data and a Dense-Point Distribution Model for Surgical Navigation," *IEEE Trans Biomed Engineering*, vol. 54, no. 12, pp. 2109-2122, Dec. 2007.

[15] Aviv Hurvitz and Leo Joskowicz, "Registration of a CT-like atlas to fluoroscopic X-ray images using intensity correspondences," *International Journal of Computer Assisted Radiology and Surgery*, vol. 3, pp. 493-504, 2008.

[16] N. Baka et al., "2D-3D shape reconstruction of the distal femur from stereo X-ray imaging using statistical shape models," *Medical Image Analysis*, vol. 15, no. 6, pp. 840-850, 2011.

[17] A.K. and Yu Zhong and Lakshmanan, S. Jain, "Object matching using deformable templates," *IEEE Transactions on Pattern Analysis and Machine Intelligence*, vol. 18, no. 3, pp. 267 -278, March 1996.

[18] C. Baegert, C. Villard, P. Schreck, L. Soler, and A. Gangi, "Trajectory optimization for the planning of percutaneous radiofrequency ablation of hepatic tumors," *Computer Aided Surgery*, vol. 12, no. 2, pp. 82-90, 2007.

[19] M.H. Chen et al., "Large Liver Tumors: Protocol for Radiofrequency Ablation and Its Clinical Application in 110 Patients Mathematic Model, Overlapping Mode, and Electrode Placement Process," *Radiology*, vol. 232, no. 1, pp. 260-271, 2004.

[20] G.D. Dodd, M.S. Frank, M. Aribandi, S. Chopra, and K.N. Chintapalli, "Radiofrequency thermal ablation," *American Journal of Roentgenology*, vol. 177, no. 4, pp. 777-782, 2001.

[21] Tobias Heimann and Hans-Peter Meinzer, "Statistical shape models for 3D medical image segmentation: A review," *Medical Image Analysis*, vol. 13, no. 4, pp. 543 - 563, 2009.

[22] Hongliang Ren and Peter Kazanzides, "AISLE: an automatic volumetric segmentation method for the study of lung allometry," in *18th International Conference on Medicine Meets Virtual Reality*, Feb. 2011.

[23] T.F. Cootes and C.J. Taylor and D.H. Cooper and J. Graham, "Active shape models - Their training and application," *Computer Vision and Image Understanding*, vol. 61, no. 1, pp. 38-59, 1995.

[24] Said Benameur et al., "3D/2D registration and segmentation of scoliotic vertebrae using statistical models," *Computerized Medical Imaging and Graphics*, vol. 27, no. 5, pp. 321-337, 2003.

[25] Peter J. Green, "On Use of the EM for Penalized Likelihood Estimation," *Journal of the Royal Statistical Society. Series B (Methodological)*, vol. 52, no. 3, pp. 443-452, 1990.

[26] Xin Kang and Russell H. Taylor and Mehran Armand and Yoshito Otake and Wai-Pan Yau and Paul Y. S. Cheung and Yong Hu, "Correspondenceless 3D-2D registration based on expectation conditional maximization," in *Medical Imaging 2011: Image-Guided Procedures, Robotic Interventions, and Modeling*, 2011, pp. 79642Z-1--8.

[27] X. Kang and W. P. Yau and Y. Otake and P. Y. S. Cheung and Y. Hu and R. H. Taylor, "Assessing 3D Tunnel Position in ACL Reconstruction Using A Novel Single Image 3D-2D Registration," in *Medical Imaging 2012: Image-Guided Procedures, Robotic Interventions, and Modeling*, 2012, pp. 831628-1--6.

[28] G.L. Nemhauser and L.A. Wolsey, *Integer and combinatorial optimization*.: Wiley New York, 1988, vol. 18.

[29] N. Aspert and D. Santa-Cruz and T. Ebrahimi, "MESH: Measuring errors between surfaces using the Hausdorff distance," in *IEEE International Conference in Multimedia and Expo (ICME)*, vol. 1, Lausanne, Switzerland, 2002, pp. 705–708.